J Muscle Res Cell Motil (2017) 38:275–289
DOI 10.1007/s10974-017-9482-8

Kinetic coupling of phosphate release, force generation and rate-limiting steps in the cross-bridge cycle

Robert Stehle[1] · **Chiara Tesi**[2]

Received: 5 July 2017 / Accepted: 12 September 2017 / Published online: 16 September 2017

Abstract A basic goal in muscle research is to understand how the cyclic ATPase activity of cross-bridges is converted into mechanical force. A direct approach to study the chemo-mechanical coupling between P_i release and the force-generating step is provided by the kinetics of force response induced by a rapid change in $[P_i]$. Classical studies on fibres using caged-P_i discovered that rapid increases in $[P_i]$ induce fast force decays dependent on final $[P_i]$ whose kinetics were interpreted to probe a fast force-generating step prior to P_i release. However, this hypothesis was called into question by studies on skeletal and cardiac myofibrils subjected to P_i jumps in both directions (increases and decreases in $[P_i]$) which revealed that rapid decreases in $[P_i]$ trigger force rises with slow kinetics, similar to those of calcium-induced force development and mechanically-induced force redevelopment at the same $[P_i]$. A possible explanation for this discrepancy came from imaging of individual sarcomeres in cardiac myofibrils, showing that the fast force decay upon increase in $[P_i]$ results from so-called sarcomere 'give'. The slow force rise upon decrease in $[P_i]$ was found to better reflect overall sarcomeres cross-bridge kinetics and its $[P_i]$ dependence, suggesting that the force generation coupled to P_i release cannot be separated from the rate-limiting transition. The reasons for the different conclusions achieved in fibre and myofibril studies are re-examined as the recent findings on cardiac myofibrils have fundamental consequences for the coupling between P_i release, rate-limiting steps and force generation. The implications from P_i-induced force kinetics of myofibrils are discussed in combination with historical and recent models of the cross-bridge cycle.

Keywords Muscle contraction · Power stroke · Tension redevelopment · Tension recovery · Myofibril force kinetics · Sarcomere dynamics

Force generation during the cross-bridge ATPase cycle: an open question

Contraction of skeletal and cardiac muscle is driven by the cross-bridge ATPase cycle. The steps generating the force and displacement in this cycle, also called the power strokes, are of particular interest. How force-generating step(s) are coupled to chemical steps in the ATPase cycle, i.e., the chemo-mechanical coupling of muscle contraction, is a central question in basic muscle research that has been continuously investigated in biochemical, biomechanical and structural studies from the molecular to the muscle level (Cooke 1997; Gordon et al. 2000; Huxley 2004; Steffen and Sleep 2004; Takagi et al. 2004; Geeves and Holmes 2005; Thomas et al. 2009; Houdusse and Sweeney 2016). An early model (Lymn and Taylor 1971) describing chemo-mechanical coupling is depicted in Fig. 1a. In the Lymn–Taylor model, force generation and product (P_i and ADP) release from the cross-bridge are merged to one-step. Subsequently, the major free energy change as well as the major transition from weak to strong actin binding states in the ATPase cycle in the cycle was assigned to the release of P_i that precedes ADP release (Trentham et al. 1972; Eisenberg and Greene 1980). These findings lead to the view in the 1980s that force-generation is coupled to P_i release (Eisenberg and Hill 1985). Neither

✉ Robert Stehle
Robert.Stehle@Uni-Koeln.de

[1] Institute of Vegetative Physiology, University of Cologne, Robert Koch Str. 39, 50931 Cologne, Germany

[2] Division of Physiology, Department of Experimental and Clinical Medicine, University of Florence, Viale Morgagni, 63, 50134 Firenze, Italy

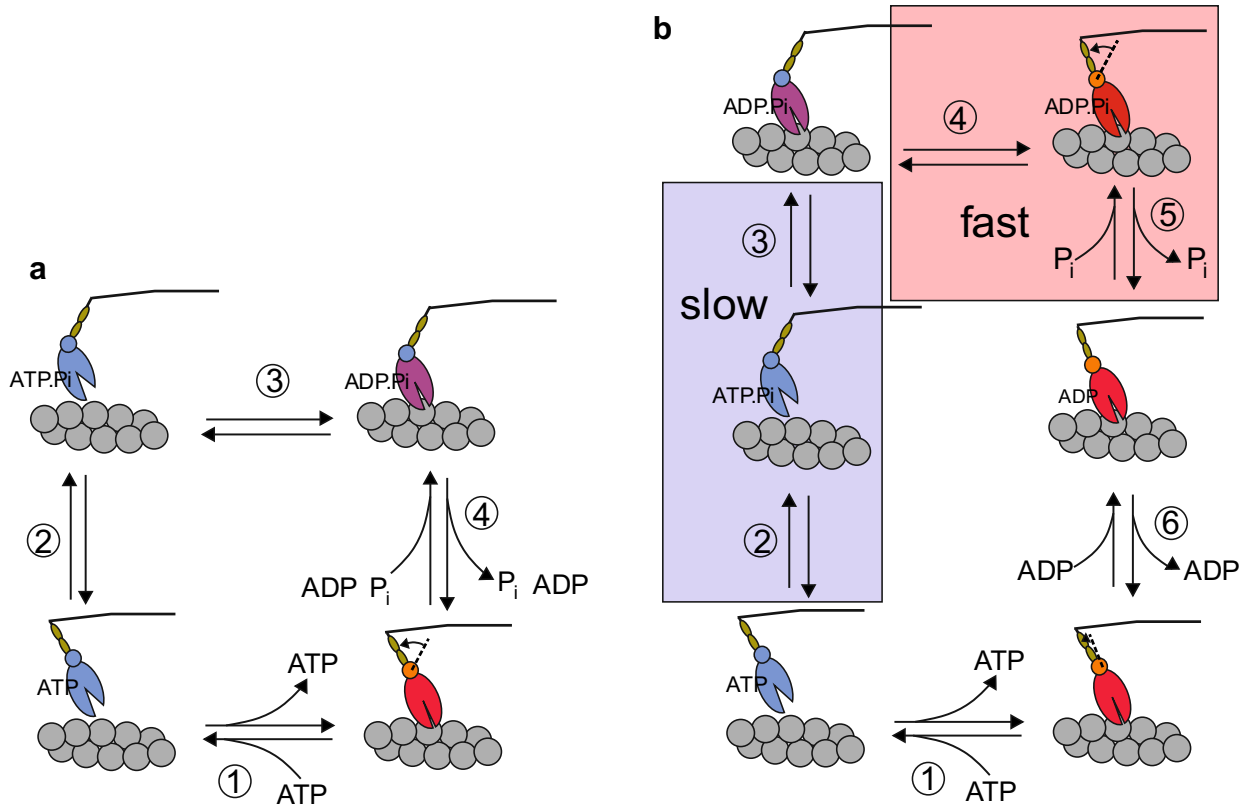

Fig. 1 Sequence of rate-limiting transitions, force-generating steps and P_i release in different models of the cross-bridge cycle. **a** Four-state model of Lymn and Taylor. **b** Extended six-state model implied from the fast force decay upon increase of [P_i]. In both models, ATP-binding induces rapid detachment of the cross-bridge from actin by opening the actin binding cleft (step 1, ①), thereby stabilizing myosin in non-force-generating states with low actin affinity (light grey coloured heads, blue colour in online version). The cross-bridge recovers the power stroke by tilting of its lever arm, and hydrolyses ATP (step 2, ②). Crucial for initiation of force generation is the preceding formation of a stereospecific, pre-force-generating AM.ADP.P_i state (mid grey coloured head, pink in online version) with a largely closed actin binding cleft (step 3, ③). Subsequent force generation is indicated by the tilt of the lever arm and the shift to dark grey colour of head (red colour in online version) and the converter domain (step 4, ④). In **a** the four-state Lymn–Taylor model, the force-generating step is inseparably coupled with release of products (P_i and ADP). Further, the model does not indicate which step(s) limit(s) the transition of cross-bridges to the force state, i.e., the transition rate *f*: ATP hydrolysis (②), formation of the pre-force-generating AM.ADP.P_i state (③) or product release (④). **b** In the extended six-state model, a fast major force-generating step (④) occurs prior to rapid P_i release (step 5, ⑤) and a further minor force-generating step with the release of ADP (step 6, ⑥). Because ④ and ⑤ present fast steps, *f* must be limited by ③ or ②. The forward transition of cross-bridges to weakly bound, non-force-generating states (rate constant *g*) is limited by the load-dependent step 6 (⑥). In absence of load, ⑥ is fast. Under high load as during isometric contraction, ⑥ is slow, so that *g* becomes similar or even lower than *f*. The isometric ATPase rate ($ATPase \sim 1/f + 1/g$) is mainly limited by *g*, whereas the rate of force redevelopment ($k_{TR} \sim f + g$) is also determined by *f*. Models modified from (Lymn and Taylor 1971) (**a**) and (Dantzig et al. 1992; Capitanio et al. 2006; Houdusse and Sweeney 2016) (**b**). (Color figure online)

the Lymn–Taylor nor the Eisenberg–Hill model differentiates whether force is generated before, during or after release of P_i. From chemical and physical principles, the view of a direct coupling, i.e., a one-step mechanism of force-generation coupled to P_i release might be simplistic. The classical view of ligand binding/dissociation is that of a rapid, diffusion-limited equilibrium that then induces a more or less slower conformational change of the enzyme. Accordingly, a two-step process of force generation coupled to P_i release is expected, i.e., a force-generating step occurring before or after a rapid P_i release. Furthermore, there might be additional slow steps in the cycle that limit the rate of force generation. The rate constant of the transition that limits the turnover of cross-bridges into force-generating states is termed *f*. If *f* represents the kinetics of an intrinsically slow process whereas force-generation and P_i release are intrinsically fast steps, *f* must belong to different step(s). The minimalist model of Lymn–Taylor was therefore refined by inserting additional steps and states, based on many kinetic and structural studies (Chalovich and Eisenberg 1982; Pate and Cooke 1989; Millar and Homsher 1990; Kawai and Halvorson 1991; Dantzig et al. 1992; Davis and Rodgers 1995; Cooke 1997; Brenner and Chalovich 1999; Gordon et al. 2000; Martin et al. 2004; Takagi et al. 2004; Geeves and

Holmes 2005; Capitanio et al. 2006; Siththanandan et al. 2006; Caremani et al. 2013; Smith 2014; Dong and Chen 2016; Geeves 2016; Houdusse and Sweeney 2016; Mansson 2016; Mijailovich et al. 2017).

To date numerous models of the cross-bridge cycle exist, which differ in many details. In particular, the sequence of the P_i release and the force-generating step is still an open debate (Llinas et al. 2015; Mansson et al. 2015; Muretta et al. 2015; Houdusse and Sweeney 2016). Furthermore, the reaction(s) and structural change(s) contributing to the rate-limiting transition f remain to be defined. Clarifying these issues is important for understanding the basic mechanism of force generation and its targeted alteration. For example, with regard to search and design of molecules targeting force production by stabilizing cross-bridges in certain chemical states, it is essential to know whether AM.ADP.P_i-intermediate(s) prior to P_i release can generate force in muscle contraction. Furthermore, understanding the nature of the transitions that determine f is essential for targeted interventions of rate-limiting steps, which provide an efficient way to tune force generation. This review focusses on the significance of mechanical studies for defining the sequence and mechanism of the rate-limiting transition f, the force-generating step and the P_i release in the cross-bridge cycle.

Kinetics of rate-limiting transitions in the cross-bridge cycle

To separate the force-generating step from the rate-limiting transition f, first one needs to know the value of f. The first model of the cross-bridge cycle by A.F. Huxley consisted of only two states, a non-force-generating and a force-generating state, and two rate constants for forward cycling, the rate constant f for entering the force-generating state and the rate constant g for leaving the force-generating state (Huxley 1957). In this model, the rate-limiting transition and the force-generating step are combined in a single step and force is proportional to $f/(f+g)$ and ATPase proportional to $f{\cdot}g/(f+g)$ or $1/f+1/g$. In the line of this seminal and prescient model, a fundamental contribution was given by B. Brenner and coworkers, based on the findings that: (1) the observed rate constant of mechanically-induced, maximally Ca^{2+} activated force redevelopment, k_{TR} probes cross-bridge turnover kinetics and reflects the sum of f and g (Brenner and Eisenberg 1986); and (2) the Ca^{2+} regulation of force generation and ATPase of isometric contracting fibres underlies rate-modulation of f, whereby f gradually increases while g remains constant with increasing the $[Ca^{2+}]$ (Brenner 1988). From the change of f it was clear that it does not present a fixed intrinsic rate constant of a single step but an apparent rate constant, termed f_{app}, of at least two steps. Brenner noted that rate-modulation of f_{app} can be explained by assuming that 'turned on and turned off forms of the regulated actin units are in a dynamic equilibrium with fast rate constants compared to cross-bridge turnover' and 'P_i release only occurs when cross-bridges are attached to the turned on form of actin'. Basically, f_{app} might result from a forward step and a foregoing faster, Ca^{2+}-regulated equilibrium modulating the initial state, A_0, of this forward step. The observed f_{app} in the experiment depends on the intrinsic rate constant $f^{\rightharpoonup}$ of the forward step as well as on the occupancy $[A_0]$ of the initial state. Noteworthy, $f^{\rightharpoonup}$ must not be slow if only very few cross-bridges are capable to undergo the forward step. Thus, it remains open whether $f^{\rightharpoonup}$ is slow and $[A_0]$ is high or whether $f^{\rightharpoonup}$ is fast and $[A_0]$ is low. The individual contributions of $[A_0]$ and $f^{\rightharpoonup}$ can be only modelled but not separately measured. Furthermore, the structural and biochemical changes contributing to the rate limiting transition f and its Ca^{2+}-modulated substitute f_{app} remain unclear. At least, the individual contributions of f_{app} and g_{app} can be derived from combined measurements of k_{TR}, force and ATPase at maximally activating $[Ca^{2+}]$ (Brenner 1988), from the Ca^{2+} dependence of force and k_{TR} (de Tombe and Stienen 2007), or from combined measurement of k_{TR}, reflecting $f_{app}+g_{app}$, and the force decay of the initial relaxation phase following rapid Ca^{2+} removal during which all sarcomeres relax isometric. The rate constant of this initial, slow, linear force decay, called 'slow k_{REL}' or 'k_{LIN}' reflects g_{app} (Poggesi et al. 2005).

Changes in the rate-limiting transitions strongly affect energy consumption. Any modification of f_{app} proportionally affects force and ATPase so that the ratio of force per ATPase, called tension cost, remains constant. In contrast, tension cost is proportional to g_{app}, as an increase of g_{app} decreases force but increases ATPase. Classical mechanical studies in single intact fibres at maximally activating $[Ca^{2+}]$ (Huxley 1957) proved that g_{app} markedly increases with shortening velocity. Strikingly, force is highly $[P_i]$-dependent, while maximum shortening velocity is hardly affected by the $[P_i]$ (Cooke et al. 1988; Caremani et al. 2015). These results indicate that P_i neither reduces force by increasing g_{app} nor by decreasing f_{app}, as proved by the positive effect of $[P_i]$ on k_{TR}. These results imply that instead of affecting the forward turnover rate f_{app}, P_i promotes the reverse turnover rate f^{-}_{app}. This view is supported by oxygen exchange measurements indicating that in isometric contracting muscle fibres, all chemical reactions from an AM.ADP-state back to an AM.ATP state are readily reversible (Hibberd et al. 1985b; Webb et al. 1986), reviewed in (Takagi et al. 2004). Thus, force reduction by P_i would result from P_i binding to an AM.ADP-state and reverse turnover via f^{-}_{app}. This $[P_i]$-dependent reverse turnover by f^{-}_{app} provides an additional exit from force-generating states to the

$[P_i]$-independent exit route via forward turnover by g_{app}. Based on the view that force redevelopment reflects overall re-distribution of cross-bridges determined by all rate-limiting transitions, in presence of P_i, $k_{TR} = f_{app} + g_{app} + f_{app}^{-}$. Recently, (Wang and Kawai 2013) reinterpreted k_{TR} to reflect only g_{app}, instead of the classical view of k_{TR} reflecting the sum of all rate-limiting transitions. However, the finding that P_i accelerates the rate of Ca^{2+}-induced force development, k_{ACT} or mechanically-induced force redevelopment, k_{TR} in fast skeletal (Hibberd et al. 1985a; Millar and Homsher 1990; Regnier et al. 1995; Regnier and Homsher 1998), slow skeletal (Millar and Homsher 1992; Wahr et al. 1997) and cardiac muscles (Araujo and Walker 1996; Edes et al. 2007) while it decreases force in proportion to the number of force-generating cross-bridges (Kawai and Halvorson 1991; Caremani et al. 2008) is strong evidence against this re-interpretation. Interestingly, in fast muscle, P_i reduces isometric ATPase to a lesser extent than force (Webb et al. 1986; Bowater and Sleep 1988; Cooke et al. 1988) while the effect is very similar in slow muscle (Potma et al. 1995; Kerrick and Xu 2004). The change of the force-ATPase ratio or tension cost by $[P_i]$ poses a complication for the modeling of P_i effect on chemo-mechanical coupling, which is still under debate (Pate and Cooke 1989; Linari et al. 2010). In summary, P_i release is reversible and $[P_i]$-dependent rebinding of P_i accelerates the redistribution amongst force-generating and non-force-generating/detached states by promoting backwards cycling.

While force redevelopment reports rate-limiting transitions in the cross-bridge ATPase cycle, force generation per se is a fast process. At the single molecule level, force rapidly develops upon attachment of myosin to actin filaments in single molecule force assays like the laser trap (Finer et al. 1994; Veigel et al. 1998; Takagi et al. 2004). Also the cross-bridge ensemble in muscle fibres can rapidly regenerate force (within several msec) after small length change perturbations (Ford et al. 1977; Kawai and Halvorson 1991; Lombardi et al. 1992; Colomo et al. 1994; Ranatunga et al. 2002; Linari et al. 2007) or pressure (Fortune et al. 1991) and temperature jumps (Davis and Rodgers 1995; Bershitsky and Tsaturyan 2002; Coupland and Ranatunga 2003). Albeit the phenomena of the rapid force recovery likely reflects a different mechanism of force generation uncoupled from or loosely coupled to the ATPase cycle (Davis and Rodgers 1995; Caremani et al. 2008, 2013), there is common consensus that not the force-generating step, but some other process or reaction, perhaps isomerization within a given force state, that limits the transition of cross-bridges to force-generating states in the ATPase cycle. To distinguish between the possible difference of force recovery and force generation coupled to ATPase cycling, the latter is termed here de novo force development. Overall, the observed broad spectra of force responses upon small and large perturbations of muscle preparations led to the hypothesis that slow transitions determine de novo force development reflected by f, while the force can be rapidly re-generated and thus the force-generating step per se could be fast.

Refinement of the force-generating mechanism coupled to P_i release in muscle fibres

The one-step mechanism of force generation along with P_i release had been accepted until the early 1990s, when seminal experiments on skinned muscle fibres using a new chemical compound, caged-P_i, produced in a new hypothesis of the two-step process for force generation (Takagi et al. 2004). Fibres were loaded with caged-P_i and the caged compound activated by flash photolysis. The photolysis caused a rapid (<1 ms) increase in $[P_i]$ in the fibre, the so called *P_i jump*, resulting in force responses with a major force reduction. The P_i-induced force response produced up to four kinetic phases (see Fig. 2b in Dantzig et al. 1992), albeit not all phases were observed in the other studies using caged-P_i (Millar and Homsher 1992; Walker et al. 1992). The sudden increase of sarcoplasmic $[P_i]$ shifts cross-bridges backwards in the cycle because it promotes P_i binding to the cross-bridge, i.e., the reversal of P_i release. Phase 1 was a short lag of several msec that was attributed to P_i binding to the AM.ADP-state and the formation of an AM.ADP.P_i-state that still generates force. Viewed in forward direction, this indicated that force is generated before P_i release. Most attention was paid to phase 2, a major exponential force decay whose kinetics were strongly $[P_i]$-dependent. The rate constant k_{Pi} of phase 2 was attributed to the kinetics of the force-generating process in the cycle and the hyperbolic form of k_{Pi} dependence on $[P_i]$ was also taken as a strong and final support to the two-step process for force generation. Beside the lag (phase 1) and the major decay (phase 2), a minor rise (phase 3) and a minor decay (phase 4) had been observed (Dantzig et al. 1992). Minor phases 3 and 4 were not studied as phase 3 was ascribed to secondary effects caused by caged compounds themselves and/or sarcomere dynamics while phase 4 was found to be highly variable and not $[P_i]$ dependent.

By the time it became possible to study P_i-induced force kinetics, the k_{TR}-measurement was already established and the kinetics of the major force decay could be compared with the rate-limiting process f_{app} probed by k_{TR}. Importantly, the force decay of phase 2 was significantly faster than the force rise induced in the k_{TR}-measurement. Thus, in fast skeletal fibres at 10–15 °C, k_{Pi} was about 2–3 times faster than k_{TR} measured at same $[P_i]$ (Millar and Homsher 1990; Walker et al. 1992). Using the caged-P_i method, k_{Pi} of phase 2 was found 2–3 times higher than k_{TR} also in cardiac

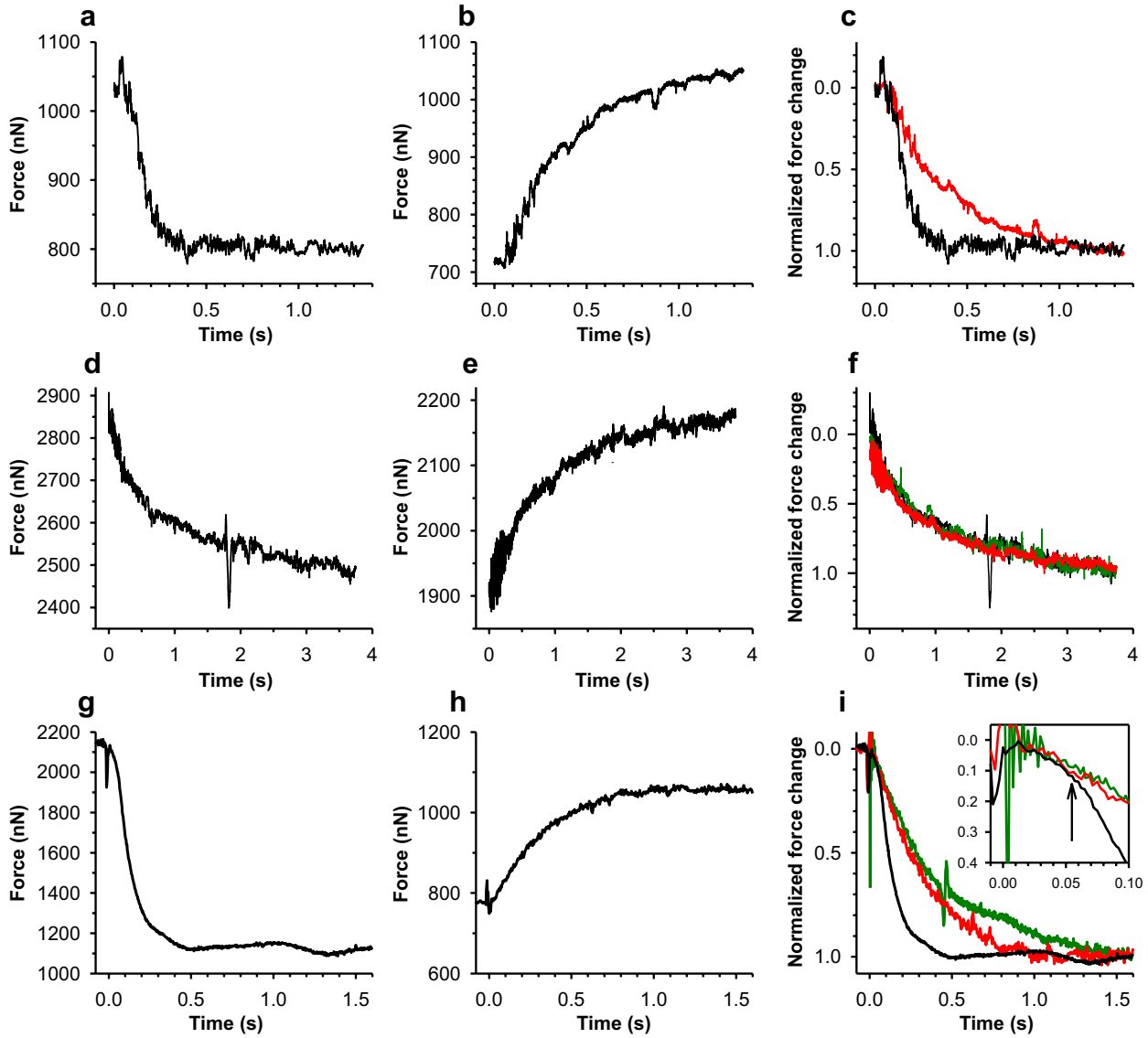

Fig. 2 Symmetry and asymmetry of force responses observed upon increases or decreases in [P_i] to the same final [P_i] during maximum Ca^{2+} activation (pCa 4.5). Force responses of myofibrils from fast skeletal muscle at 5 °C (upper row, **a**–**c**), slow skeletal muscle at 15 °C (mid row, **d**–**f**), and cardiac myofibrils at 10 °C (lower row, **g**–**i**) were induced by rapid increase of [P_i] (left column, **a, d, g**) or rapid decrease of [P_i] (mid column, **b, e, h**). At time = 0, the [P_i] was changed (in mM) from 0.2 to 1 (**a**), 5 to 1 (**b**), 0.2 to 2 (**d**), 20 to 2 (**e**), 0.2 to 10 (**g**), and 20 to 10 (**h**). Graphs in the right column (**c, f, i**) illustrate force transients from the respective row after normalization to amplitude and direction, i.e., force rises were inverted to enable comparison of kinetics with force decays. Circles (red lines in online version) are normalized force changes upon decrease in [P_i]. Triangles (green lines in online version) are normalized force changes in k_{TR}-measurements performed at the corresponding [P_i], i.e. at the final [P_i] in the P_i jump experiments. Note the asymmetry of force rise and force decay when changing to the same [P_i] in fast psoas (**c**), whereas there is symmetry in the slow soleus (**f**). In cardiac myofibrils, there is initial symmetry during upon the [P_i] change (best seen by the magnification of the initial part in the inlet), turning to asymmetry at the time of the transition from the first, minor force decay to the second, major force decay upon increase of [P_i] (black lined transient). The arrow marks the duration of phase 1 ($t_{+Pi(1)} = 57$ msec) obtained by fitting the black transient with the biphasic function used in (Stehle et al. 2002a; Stehle 2017). The similar slopes of the normalized force changes before $t_{+Pi(1)}$ illustrate the symmetry of $k_{+Pi(1)}$ and k_{-Pi} and similarity with k_{TR} (for more data, see (Stehle 2017) and Fig. 3c). Asymmetry starts with the onset of the major second phase (see higher values of $k_{+Pi(2)}$ compared to and k_{-Pi} and k_{TR} in Fig. 3c). (Color figure online)

muscle at 15 °C (Araujo and Walker 1996). This result was interpreted to mean that there is a fast force-generating step closely associated to P_i release that can be dissected from the slower rate-limiting transitions reflected by *f*. The [P_i]-dependence of the kinetics indicated that this force-generating step is a fast isomerization prior to P_i release, i.e., that force generation occurs in the ADP.P_i-bound state of the cross-bridge. The forward and backward rate constant

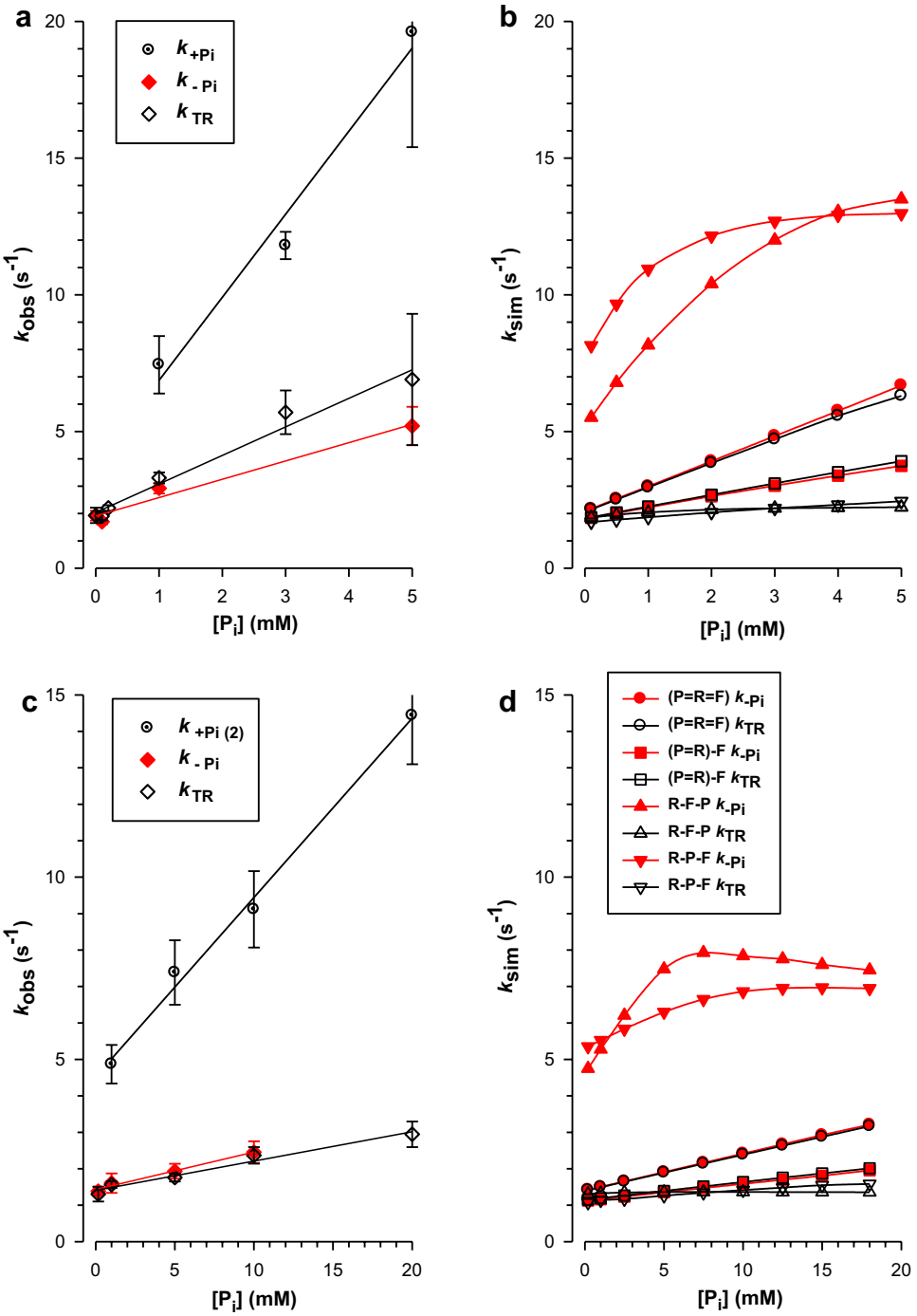

of this force-generating isomerization step were derived from the hyperbolic dependence of k_{Pi} versus the [P_i]. In fast skeletal muscle fibres, the forward rate constant of this step was markedly higher than f_{app}. In consequence, refined cross-bridge models consisted of a reversible, force-generating step that occurs after a slower, rate-limiting step or transition (related to f) and before rapid P_i release in the cross-bridge cycle (Fig. 1b). The finding of the fast force decay after a jump increase in [P_i] were convincing because the kinetic behavior of the P_i transient was consistent with the sequential reaction involving a rapid equilibrium of P_i release/rebinding and a slower reversible force-generating step exhibiting a saturation as the substrate is increased. The sequence of these three key events in the cross-bridge cycle seemed to be solved even if contemporaneous caged-P_i studies in slow muscle cast a shadow on this hypothesis. Measurements of k_{Pi} and k_{TR} in soleus fibres at same [P_i] and at maximally activating [Ca^{2+}] showed that P_i release could

◂**Fig. 3** Measured and simulated [P_i]-dependence of force kinetic parameters. **a** Rate constants obtained in experiments on fast skeletal rabbit psoas myofibrils (fs-mf) at 5 °C. **c** Rate constants obtained in experiments on cardiac myofibrils (c-mf) from guinea pig left ventricle at 10 °C (Stehle 2017). Experimentally observed rate constants in **a** and **c** were determined at full Ca^{2+} activation (pCa 4.5). The rate constant of the force rise upon rapid decrease of [P_i], k_{-Pi} is indicated by filled diamonds (red in online version). The rate constant of mechanically-induced force redevelopment, k_{TR} is indicated by open diamonds. The rate constant of the major force decay upon rapid increase of [P_i] that refers to the rate constant of the total force decay in fs-mf (k_{+Pi} in **a**) and to the rate constant of the second, major phase of force decay in c-mf ($k_{+Pi(2)}$ in **c**) is indicated by dotted circles. For an illustration of the bi-phasic force decay in c-mf, see Fig. 2i. Note the similar [P_i] relations of k_{TR} and k_{Pi} and their difference to k_{+Pi} or $k_{+Pi(2)}$. **b, d** [P_i]-dependences of parameters obtained in model simulations matched to the fs-mf and c-mf experiments in a and c, respectively. For each myofibril experiment, four model versions differing in the sequence of the rate-limiting transition '*f*' (R), the force-generating step (F) and P_i release step (P) (models: R→F→P, R→P→F, P=R→F, P=R=F) were tested for their ability to reproduce the observed [P_i]-dependence of k_{TR} and k_{-Pi}. Model simulations indicated by R→F→P (relations marked by triangles with tips *up*) in **b** and **d** refers to the six-step model depicted in Fig. 1b, i.e. the sequence R, F and P with fast force-generation before fast P_i-release. In this model, the first force-generating state is an ADP.P_i-state after step 4. Intrinsic rate constants used for R→F→P model: Step 1 (ATP-binding): k_{+1} = 220 s^{1} (fs-mf), 200 s^{-1} (c-mf); step 2 (ATP hydrolysis): k_{+2} = 15 s^{-1} (fs-mf), 10 s^{-1} (c-mf); k_{-2} = 1.2 s^{-1} (fs-mf), 2 s^{-1} (c-mf); step 3 (R): k_{+3} ('*f*') = 1.6 s^{-1} (fs-mf), 1.0 s^{-1} (c-mf); k_3 ('*f*'') = 1.6 s^{-1} (fs-mf), 1.0 s^{-1} (c-mf); step 4 (F): k_{+4} = 16 s^{-1} (fs-mf), 10 s^{-1} (c-mf); k_{-4} = 16 s^{-1} (fs-mf), 10 s^{-1} (c-mf); step 5 (P): k_{+5} (P_i release) = 16 s^{-1} (fs-mf), 10 s^{-1} (c-mf); k_{-5} (P_i rebinding) = 9 mM^{1} s^{1} (fs-mf), 1 mM^{-1} s^{-1} (c-mf); step 6 (ADP release) k_{+6} (*g* at isometric contraction) = 0.5 s^{-1} (fs-mf and c-mf), k_{+6} (*g* at unloaded contraction) = 50 s^{-1} (fs-mf and c-mf). To simulate k_{TR}-measurements (open symbols), [P_i] was kept constant and *g* switched from unloaded (k'_{+6}) to isometric contraction (k_{+6}). To simulate k_{-Pi}-measurements (filled symbols, red coloured in online version), k_{+6} was kept isometric (0.5 s^{-1}), and [P_i] switched from 10 mM P_i (fs-mf) or 20 mM P_i (c-mf) to the indicated [P_i]. To simulate a model with sequence R → P → F and fast force-generation after fast P_i release (relations marked by triangles with tips down), the rate constants of R → F → P model were kept but the sequence of F and P was interchanged. Thus, in R → P → F model, step 4 = P, step 5 = F and the first force-generating state is an ADP-state. The model (P = R) → F (relations marked by squares) presents simulations for rate-limiting P_i release and subsequent fast force-generation: step 3 (R) and step 4 (P) of the R → P → F model were merged to a single, slow step with the forward rate constant $k_{+(4=3)}$ = 1.6 s^{-1} (fs-mf) or 1.0 s^{-1} (c-mf) and the reverse rate constant $k_{-(4=3)}$ = 0.9 mM^{-1} s^{-1} (fs-mf) or 0.1 mM^{-1} s^{-1} (c-mf). For model simulations indicated by P = R = F (relations marked by circles), P_i release, force-generating and rate-limiting step, i.e., all steps 46 in the R → F → P model are merged to a single, slow step with forward rate constant [$k_{+(3=4=5)}$] = 1.6 s^{-1} (fs-mf) or 1.0 s^{-1} (c-mf), and reverse rate constant [$k_{-(3=4=5)}$] = 0.9 mM^{-1} s^{-1} (fs-mf) or 0.1 $mM^{-1}s^{-1}$ (c-mf). (Color figure online)

not be always 'dissected' from the slower rate-limiting transitions reflected by *f* as this difference was clearly temperature dependent and almost disappeared at 10 °C (Millar and Homsher 1992). As highlighted in the following chapters, the sequence and mechanistic relation of the three events is a still controversially discussed unsolved problem.

Re-exploration of the force-generating mechanism coupled to P_i release in myofibrils

At the end of the 1990s, an important advancement for the study of the non-steady-state effects of [P_i] on force kinetics came from mechanical measurements in striated muscle myofibrils which are in rapid diffusional equilibrium with the bathing medium and suitable for mechanical measurements (Colomo et al. 1997, 1998). With single or thin bundles of myofibrils (1–3 μm wide), concentrations inside the myofilament lattice can be rapidly and precisely modified without the use of caged compounds but simply by rapid alternation of perfusion fluxes. This made it possible to resolve the kinetics of isometric force rise and relaxation in calcium activation cycles as well as the kinetics of force transients initiated by P_i jumps (Tesi et al. 2000). A real advantage of myofibril P_i jumps over caged-P_i skinned fibre experiments is the ability to precisely change [P_i] in a much wider and controlled range and observe not only the decrease in force following sudden [P_i] increase but also the reverse, i.e., force increase following sudden [P_i] decrease. When submitted to rapid jumps in [P_i], single or thin bundles of rabbit psoas myofibrils (5 °C; Fig. 2a, c) responded with sudden changes in force and the kinetics of both the force decrease which followed the increase in [P_i] (rate constant k_{+Pi}) and of the force increase following the decrease in [P_i] (rate constant k_{-Pi}) were measured.

As previously observed in skinned fibres with caged-P_i, k_{+Pi} was scarcely affected by the activation level and about three times faster than the rate of Ca^{2+}-induced force development k_{ACT}, or mechanically-induced redevelopment k_{TR}, measured at the same final [P_i]. Taking in account differences in experimental temperature, absolute values of k_{+Pi} were similar to those previously observed in caged-P_i force transients in skinned fibres but the dependence on final [P_i] showed no sign of saturation in the range of measurements, as expected from a two-step mechanism. Anyway, based on the close correspondence with caged-P_i findings (estimated second order binding constant) and on the steady-state effect of [P_i] on isometric force, showing a definite plateau at high [P_i] (Tesi et al. 2002a), authors favoured cross-bridge models in which force is produced by an isomerization of AM.ADP.P_i complex immediately preceding a fast and non-rate-limiting P_i release step. Unexpectedly from a two-step mechanism of force-generation and P_i release like depicted in Fig. 1b, rabbit psoas myofibril experiments reported that the force increase following the reversal of the jump was slower, i.e., its rate constant k_{-Pi} was much less than k_{+Pi}, whereas k_{-Pi} was undistinguishable from k_{TR} measured at the same final [P_i] (Figs. 2a, c, 3a; Table 1, Tesi et al. 2000). Both k_{-Pi} and k_{TR} have not only the same values but also the same calcium, [P_i] and temperature dependencies, which are

Table 1 Kinetics of P_i jumps, force redevelopment and relaxation in different myofibril preparations at contaminant (0.2 mM) and 2–5 mM [P_i] in full activation solution (pCa 4.5)

Myofibril type conditions	Force generation	P_i jump (–)	Relaxation		P_i jump (+)	
	k_{TR} (s^{-1})	k_{-Pi} (s^{-1})	Slow k_{REL} (s^{-1})	Fast k_{REL} (s^{-1})	$k_{+Pi(1)}$ (s^{-1})	k_{+Pi} or $k_{+Pi(2)}$ (s^{-1})
Rabbit psoas 0.2 mM P_i (5 °C)	2.7 ± 0.1 (25)[a]	1.7 ± 0.1 (5)[f]	0.6 ± 0.03 (51)[a]	17.7 ± 1.1 (51)[a]	n.d.	n.d.
Rabbit psoas 5 mM P_i (5 °C)	5.4 ± 0.6 (13)[b]	5.2 ± 0.7 (13)[b]	3.4 ± 0.36 (15)[a]	13.9 ± 1.4 (15)[a]	n.d.	18.2 ± 2.0 (13)[b]
Rabbit soleus 0.2 mM P_i (15 °C)	2.1 ± 0.3 (12)[a]	n.d.	0.3 ± 0.04 (13)[a]	2.1 ± 0.2 (13)[a]	n.d.	n.d.
Rabbit soleus 2 mM P_i (15 °C)	1.8 ± 0.2 (6)[b]	1.8 ± 0.2 (6)[b]	0.8 ± 0.1 (8)[c]	5.8 ± 0.5 (8)[c]	n.d.	3.2 ± 0.2 (6)[b]
Guinea pig, cardiac 0.2 mM P_i (10 °C)	1.3 ± 0.2 (9)[d]	1.4 ± 0.1 (9)[d]	0.7 ± 0.1 (32)[e]	10.9 ± 0.4 (32)[e]	n.d.	n.d.
Guinea pig, cardiac 5 mM P_i (10 °C)	1.9 ± 0.2 (9)[d]	1.8 ± 0.1 (9)[d]	1.9 ± 0.5 (7)[e]	18.7 ± 2.3 (7)[e]	1.8 ± 0.2 (6)[d]	7.4 ± 0.9 (6)[d]

Mean ± SEM, number in parentheses = *n*

[a]Tesi et al. (2002b)

[b]Tesi et al. (2000)

[c]Belus et al. (2003)

[d]Stehle (2017)

[e]Stehle et al. (2002a)

[f]Unpublished

different from those of k_{+Pi} (Tesi et al. 2000; Piroddi et al. 2003).

The interpretation of the unexpected marked asymmetry of the rate of force change when a given final [P_i] is approached from a higher versus a lower [P_i] posed then a serious problem of interpretation. Poggesi, Tesi and coworkers (Tesi et al. 2000, 2002a) tested the possible role of experimental systematic artifacts, mainly due to lack of control of mechanical conditions of myofibrils during contraction, but results of ADP or Ca^{2+} jumps showed that the asymmetry in the kinetics of declining or rising force transients was present only in P_i jumps. At the same time, attempts to fit this behavior with current models of cross-bridge action failed (Smith and Sleep 2006). An interesting point came from experiments performed with rabbit soleus myofibrils which confirmed the close correspondence of the kinetics of the transient rise in force initiated by a sudden decrease in [P_i] and k_{TR} but reported the asymmetry in force kinetics following P_i jumps in opposite directions only at 20 °C. At 15 °C, the difference between k_{+Pi}, k_{-Pi} and k_{TR} were greatly reduced and in some cases all the rates superimposed on k_{TR}, as shown in Fig. 2d–f. This observation is in line with previous results from caged-P_i experiment in soleus muscle, reporting a marked temperature dependence of k_{+Pi} which at 10 °C was also found almost indistinguishable from k_{TR} (Millar and Homsher 1992). The explanation given at the time by Homsher and coworkers was that in slow muscle, depending on temperature, 'the force generating and P_i release steps are not kinetically isolated from the rest of the cycle as is the case in fast twitch muscle fibres' and the P_i release itself is part of the rate limiting step(s) of the cross-bridge chemo-mechanical cycle. In conclusion, experiments in rabbit skeletal myofibrils re-opened the question about the one step/two steps coupling of P_i release with force generation and the assignment of the overall rate-limiting step.

Recently, a possible resolution of the puzzle posed by the asymmetry in P_i jumps came from the investigation of force responses and individual sarcomere dynamics upon rapid increase or decrease in P_i in maximally Ca^{2+} activated guinea pig cardiac myofibrils (Stehle 2017). This study showed that in this experimental model (10 °C), the force decay upon rapid increase in [P_i] is clearly biphasic with an initial slow decline [phase 1; $k_{+Pi(1)}$] and a subsequent three to fivefold faster major decay [phase 2; $k_{+Pi(2)}$]. The kinetics of this major second phase corresponded to the kinetics of the major fast phase detected in both fast skeletal muscle skinned fibres and myofibrils. As previously observed in skeletal myofibrils, also here the kinetics of the rise in force following P_i decrease was monophasic (k_{-Pi}) and had the same rate as k_{TR} or k_{ACT} at the same final ligand concentration. Interestingly, the monitoring of individual sarcomeres of 'isometrically' held myofibrils induced by P_i jumps showed that sarcomere dynamics during force change was present only upon rapid increase in [P_i], starting with an individual sarcomere give triggering fast phase 2. This behavior closely matches the sarcomere dynamics taking

place in guinea pig cardiac myofibrils during the fast phase of force relaxation following calcium removal (Stehle et al. 2002a; Telley et al. 2006), both for the absolute kinetics and $[P_i]$ dependence. Interestingly, the force kinetics of the other phases ('truly isometric') were found reasonably symmetric, with the rate constant of the initial slow decline upon rapid increase in $[P_i]$ $k_{+Pi(1)}$ as slow as k_{-Pi} or k_{TR} and dependent only on the final $[P_i]$ (Stehle 2017). These results strongly suggest that, at least in cardiac myofibrils, the asymmetry arises from sarcomere dynamics, speeding up the force decrease transient by the superimposition of a relaxation-like process (Stehle et al. 2002a; Tesi et al. 2002b; Poggesi et al. 2005). k_{-Pi} or k_{TR} would then better reflect the overall sarcomere cross-bridge kinetics and its $[P_i]$ dependence, suggesting that P_i release cannot be separated from the rate-limiting transition leading to force-generating states in the chemo-mechanical cycle.

How then to reconcile these findings with previous P_i jumps in skeletal muscle myofibrils and skinned fibres? The main problem is raised by fast skeletal muscle, as in slow muscle, depending on temperature, it is possible to find conditions were P_i jump kinetics comes close (Millar and Homsher 1992; Tesi et al. 2000) or even superimposes to k_{TR} without asymmetry (Fig. 2f). In rabbit psoas myofibrils, many different tests (Ca^{2+} jumps, ADP and BDM jumps; Tesi et al. 2000) were employed to rule out the possibility that mechanical artifacts and sarcomere dynamics could be the origin of the marked asymmetry of the rate of force changes when a given final $[P_i]$ is approached from a higher versus a lower $[P_i]$. Results of these experiments showed that the asymmetry in the kinetics of rising or declining force transients was present only in P_i jumps. Moreover, a relaxation-like behavior in P_i jumps to final increased $[P_i]$ was excluded mainly based: (1) on the lack of effect of initial $[P_i]$ and force on the kinetics of P_i jumps, and (2) on the strong P_i dependence of k_{+Pi} versus an almost P_i insensitive fast phase relaxation in psoas muscle at 5 °C (Tesi et al. 2002b) and Table 1. Unfortunately, the resolution of P_i jumps experiments in rabbit psoas myofibrils at low temperature was limited by a substantial mechanical artifact on pipette movement that together with the dead time of solution change could have masked or blurred the possible presence of an initial linear phase of relaxation. However, in this case the delay is expected to last much longer than the mechanical artifact of about 80–90 msec at 5 mM final $[P_i]$ (Tesi et al. 2002b) and Table 1.

Does in rabbit psoas myofibrils the *apparent* monophasic behavior of k_{+Pi}, its 3–4 times higher value than k_{TR} at maximally activating $[Ca^{2+}]$ and its high $[P_i]$ dependence arise by switching from isometric P_i jumps of small amplitude (low $[P_i]$) to conditions progressively dominated by relaxation-like behaviour and fast k_{REL} (high $[P_i]$)? Should this happen, then P_i release step would match the rate-limiting transition *f* of cross-bridge cycle assayed by k_{TR}. But another possibility is that depending on experimental model (fast or slow muscle) or conditions ($[P_i]$, temperature, initial force), the applied perturbation probes an event, i.e. P_i release step or P_i release associated step, that is (or is not) rate-limiting for the overall cross-bridge cycle. If the latter is the case, then it needs to be determined which mechanism other than sarcomere dynamics can explain the asymmetry of k_{+Pi} and k_{-Pi}, and why k_{-Pi} is similar to k_{TR}. These questions remain open and further experiments are needed to asses these points, combining force and sarcomere dynamics measurements during P_i jumps in fast skeletal myofibrils.

Comparison of force kinetics and sarcomere dynamics upon changes in $[P_i]$ and $[Ca^{2+}]$

In myofibril preparations from fast skeletal, slow skeletal, and cardiac muscles, rapid decreases in $[P_i]$ and rapid increases in $[Ca^{2+}]$ induce mono-phasic slow force rises (Tesi et al. 2000, 2002a; Stehle 2017). While the force decay during full relaxation induced by complete Ca^{2+} removal is clearly biphasic in all these myofibril preparations (Poggesi et al. 2005), the biphasic behaviour of force decay after the increase in $[P_i]$ is only clearly seen in cardiac myofibrils (Stehle 2017) and remains uncertain for skeletal myofibrils (Fig. 2). In cardiac myofibrils there is a strikingly similar pattern of sarcomere dynamics occurring during the second, fast phases of force decays upon rapid increase of $[P_i]$ and rapid decrease of $[Ca^{2+}]$ (Stehle et al. 2002a; Stehle 2017). Cardiac myofibrils from guinea pig are a preferential preparation to resolve the spatial–temporal behaviour of sarcomere dynamics because of the slow myosin isoform and the discrete length change behaviour of individual sarcomeres. In both situations, upon increase of $[P_i]$ and upon decrease of $[Ca^{2+}]$, the transition from the slow first phase to the fast second phase in the biphasic force decay coincides with the onset of rapid lengthening, i.e., with the onset of 'give', of a single, weak sarcomere, whereupon the give propagates from one sarcomere to the next along the myofibril. As discussed below, besides some differences arising from inactivation of cross-bridge attachment after Ca^{2+} removal and load dependence of sarcomere dynamics, the corresponding phases in P_i jump and relaxation experiments observed in cardiac myofibrils (Stehle et al. 2002a; Stehle 2017) are based on similar rates in the cross-bridge cycle.

Similarities of force rises upon $[P_i]$ and $[Ca^{2+}]$ changes and their implications

As indicated by their similar rate constants, force rises induced by decrease in $[P_i]$ (k_{-Pi}), increase in $[Ca^{2+}]$ (k_{ACT}) and slack-restretch (k_{TR}) occur with very similar kinetics

determined by the transitions in the cycle limiting redistribution of cross-bridges among non-force and force-generating states (Figs. 2, 3), (Stehle et al. 2009; Stehle 2017). Thus, all these force rises primarily reflect cross-bridge turnover kinetics and even the force rise in k_{ACT}-measurements seems to be little further limited by the additional Ca^{2+} activation of the thin filament in comparison to k_{TR}-measurements, a common finding in myofibrils and fibres from skeletal and cardiac muscles (Wahr and Rall 1997; Palmer and Kentish 1998; Stehle et al. 2002a, b; Tesi et al. 2002a, b), and consistent with Ca^{2+} rapidly switching on troponin in skeletal and cardiac myofibrils (Solzin et al. 2007; Lopez-Davila et al. 2012). The observed rate constants of all three type of force rise reflect the sum of apparent rate constants of cross-bridge turnover from non-force-generating to force-generating states (f_{app}) and from force-generating to non-force states via backwards (f^-_{app}) and forwards (g_{app}) cycling, respectively. f_{app} increases with increasing $[Ca^{2+}]$, f^-_{app} increases with stretch and increasing $[P_i]$, while g_{app} mainly increases with lowering the load and increasing shortening velocity. In the absence of sarcomere dynamics, $k_{obs} = f_{app}([Ca^{2+}]) + f^-_{app}([P_i]) + g_{app}$, where k_{obs} can be k_{-Pi}, k_{TR} or k_{ACT}, and f_{app}, f^-_{app} and g_{app} adopt values near the isometric contraction condition. Under this condition, both $f^-_{app}([P_i])$ and g_{app} approach low values, leading to slow turnover of cross-bridges out of force-generating states and a high duty ratio ($f_{app}/(f_{app} + f^-_{app} + g_{app})$).

Differences of force decay upon $[P_i]$ and $[Ca^{2+}]$ changes and their implications

The kinetics of the initial, slow force decay following rapid Ca^{2+} removal is consistent with a rapid switch-off of the regulatory troponin-tropomyosin system, rapidly preventing de novo formation of force-generating cross-bridges (Stehle et al. 2002a; Tesi et al. 2002b; Poggesi et al. 2005). Because f_{app} rapidly decreases close to zero, the rate constant of the initial, linear slow relaxation phase, slow k_{REL}, during which sarcomeres and half-sarcomeres remain isometric (Stehle et al. 2002a; Telley et al. 2006), reflects $f^-_{app}([P_i]) + g_{app}$. This is different to the rate constant $k_{+Pi(1)}$ of the initial slow force decay following rapid increase of $[P_i]$ observed in cardiac myofibrils, where $[Ca^{2+}]$ remains constantly high and f_{app} maintains at the former value. Thus, $k_{+Pi(1)}$ like k_{-Pi} reflects $f_{app} + f^-_{app}([P_i]) + g_{app}$. Because only f^-_{app} but not f_{app} changes with the $[P_i]$, the dependences of k_{-Pi} and $k_{+Pi(1)}$ versus the $[P_i]$ reveals the function $f_{app}([P_i])$. k_{-Pi} increases linearly with $[P_i]$, at rates of 0.9 s^{-1} per mM P_i in fast skeletal myofibrils and 0.1 s^{-1} per mM P_i in cardiac myofibrils (Tesi et al. 2000; Stehle 2017) (Fig. 3a, c). Linear $[P_i]$-dependences are also observed for $k_{+Pi(1)}$ in cardiac myofibrils (Stehle 2017) and k_{+Pi} in slow skeletal myofibrils, especially at low temperature (Tesi et al. 2000). This suggests that f_{app} increases in proportion to $[P_i]$, i.e., $f^-_{app}(\cdot[P_i]) = \text{const}\cdot[P_i]$. Such a linear function is expected with force reduction induced by P_i rebinding being coupled to a rate-limiting transition in the cross-bridge cycle as seen by the simulated relations between k_{-Pi} and $[P_i]$ for the models termed P = R = F and (P = R) → F described in Fig. 3b, d.

In cardiac myofibrils, the values of f^-_{app} and g_{app} dramatically increase with the onset of sarcomere give and the beginning of the second major fast phase of force decays during relaxation or upon the increase of $[P_i]$ reflected by the high values of their rate constants fast k_{REL} and $k_{+Pi(2)}$, respectively (Stehle et al. 2002a; Stehle 2017). Because $k_{+Pi(2)}$ correlates with the propagation rate of sarcomere give and $k_{+Pi(2)}$ decreases when the amplitude of the force change is reduced by switching from different initial $[P_i]$ to the same final $[P_i]$, the rate of cross-bridge detachment during sarcomere give is likely affected by the amplitude of the force change. The latter could also explain why in cardiac myofibrils $k_{+Pi(2)}$ is lower than fast k_{REL} measured at same $[P_i]$, because relaxation from full activation causes a large force decay. From a mechanistic point of view, sarcomere give during relaxation and upon P_i jump can both be explained by give stretching cross-bridges and accelerating cross-bridge detachment via faster backwards cycling, i.e., by increasing f^-_{app}. This view is supported by the findings in fibre studies that stretch rapidly reduces the rate of P_i release, inducing redistribution of cross-bridges towards ADP.P_i-binding states (Mansfield et al. 2012). The fast cross-bridge detachment in the lengthening (give) sarcomeres reduces the load in the serially connected other sarcomeres and therein promotes cross-bridge detachment via fast forwards cycling by increasing g_{app} (Stehle et al. 2009). Furthermore, temporal and spatial sequence of give is directed by compliance of serial and transversal structures that connect the cross-bridge registers of the half-sarcomeres (Telley and Denoth 2007; Campbell 2016).

One difference in sarcomere dynamics during relaxation after Ca^{2+} removal and sarcomere dynamics increase of $[P_i]$ is the shortening of sarcomeres before their give. In complete relaxations, sarcomere shortening is very small (Poggesi et al. 2005) and amounts in average to less than 5 nm per half sarcomere (Telley et al. 2006). Negligible sarcomere shortening during relaxation indicates that cross-bridges cannot reform new interactions due to rapid inactivation upon Ca^{2+} removal and cannot drive filament sliding beyond a critical distance limited by the

interactions existing at Ca^{2+} removal. Because the myofibril is fixed at its ends and overall length remains almost constant, the lengthening of sarcomere give during relaxation is mainly balanced by shortening of passive compliant sarcomeres at the ends while the inner segment lengthens (Telley et al. 2006). In contrast, after a P_i jump, cross-bridges can still reform continuously force-generating interactions and sarcomeres actively shorten by ~100 nm before give spreads to them (see Fig. 3a in Stehle 2017). In this case, give of individual sarcomeres is almost fully balanced by shortening of the Ca^{2+}-activated sarcomeres in the inner segment, which hardly changes in total and mean sarcomere length. This explains why no sarcomere dynamics has been detected by measurement of mean sarcomere length in P_i jump experiments (Dantzig et al. 1992), whereas the role of sarcomere give for initiating rapid relaxation has been early recognized (Edman and Flitney 1982).

Significance of slow force response upon [P_i] decrease for the cross-bridge mechanism

The fundamental role of the P_i release for limiting the rate of contraction becomes very evident, when the kinetics of a force rise induced by a rapid decrease of [P_i] (rate constant k_{-Pi}) is compared with the de novo force generation induced by a rapid increase of [Ca^{2+}] (rate constant k_{ACT}) or a large mechanical perturbation (rate constant k_{TR}). Force rises induced by [P_i]-decreases and [Ca^{2+}]-increases are monophasic exponential and exhibit the same kinetics (Tesi et al. 2000; Stehle 2017). At same final [P_i] and [Ca^{2+}], the rate constants k_{-Pi} and k_{TR} are the same, (Fig. 3a, c; Table 1). Ca^{2+} induces force generation de novo from the relaxed state, requiring conformational changes for activation of the thin filament and conformational changes in the myosin head for formation of a stereospecific myosin-actin interaction. The latter Ca^{2+}-regulated transitions in the cross-bridge cycle usually are assumed to occur before P_i release and to limit the rate of force generation, whereas P_i release and force-generating step per se are regarded to be fast events. Thus P_i release/rebinding is usually considered to be a rapid equilibrium (Kawai and Halvorson 1991; Dantzig et al. 1992; Takagi et al. 2004). Aside from this there is ongoing discussion about the sequence of the P_i release step and the force-generating step (Llinas et al. 2015; Muretta et al. 2015). The finding that rapid decrease of [P_i] induces the same slow force rise as de novo force generation rules out sequential models of a slow rate-limiting transition preceding a fast force-generating step coupled to rapid P_i release, regardless of whether first the force is generated or the P_i is released (Stehle 2017). This conclusion is corroborated by the simulated [P_i] dependences of k_{-Pi}- and k_{TR} at maximally activating [Ca^{2+}] for different model scenarios (Fig. 3b, d). Model scenarios involving a fast force-generating step either before or after fast P_i release (models termed R →F → P and R → P → F in Fig. 3b, d) predict higher values of k_{-Pi} compared to k_{TR}, in contrast with the similar values of k_{-Pi} and k_{TR} observed in fast skeletal and cardiac myofibrils experiments. Such models also fail to reproduce the strong rate modulation of k_{TR} by [P_i] observed in experiments (Fig. 3a, c). Thus, uncoupling of P_i°release/rebinding from the rate-limiting forward/backwards transitions f and f^- results in nearly flat relations of k_{TR} versus the [P_i] (simulations of R → F → P and R → P → F models in Fig. 3b, d). In contrast, assigning P_i release/rebinding the rate-limiting transitions f and f^- (models termed P = R = F and (P = R)→F in Fig. 3b, d) yields similar values of k_{-Pi} and k_{TR} as observed in the myofibril experiments (Fig. 3a, c). Interestingly, these models also produce two further features evident in myofibril experiments, i.e., (1) strong rate-modulation of k_{TR} by [P_i], and (2) linear relation of k_{-Pi} versus [P_i]. In summary the similarity of k_{-Pi}, k_{TR} and k_{ACT} at maximally activating [Ca^{2+}], and the [P_i]-dependences of k_{-Pi} and k_{TR} indicate that upon perturbing the P_i release/P_i binding equilibrium, the cross-bridges have to pass the same rate-limiting transition as they do when force is generated de novo, either upon large scale mechanical perturbation as well as upon Ca^{2+} activation. The simplest explanation for this would be that P_i release/rebinding is tied to a slow, fully reversible conformational change in the cross-bridge controlled by Ca^{2+} activation of the thin filament.

Force kinetics upon [P_i]-decrease reflecting rate-limiting steps also set a new criterion for extended models that contain multiple force-generating states for straightforwardly integrating the rapid force recovery after small length change into the ATPase cycle (Caremani et al. 2013). Although the force-generating steps can occur repetitively, uncoupled, independent from P_i release in this model, they still involve a fast isomerization step coupled to rapid P_i release for priming the ability of cross-bridges to undergo these force-generating steps. Such a fast priming step still predicts faster force responses upon [P_i] changes than observed in k_{TR}-measurements. Again, to overcome this problem, the P_i release must be coupled to a rate-limiting transition with slow rate f.

The slow force responses upon [P_i] changes can be explained in either way, but each of them requires exceptional assumptions. One of them is that [P_i] modulates the force per cross-bridge rather than the number of cross-bridges. This relates to the idea that the energy transformation of P_i release into force generation is an irreversible step whereby the [P_i] determines the average force per cross-bridge rather than the time a cross-bridge spends in force-generating states; i.e. rather than the duty ratio. This explanation is very unlikely because recent fine mechanical measurements in skinned fibres that take filament

compliance into account showed that force per cross-bridge is little or not affected by the [P_i] (Caremani et al. 2008). The rate-modulation of k_{TR} by [P_i] supports the alternative explanation of high [P_i] lowering the duty ratio via increasing the rate constant f^-_{app} of backwards cycling according to a two-step mass action model, i.e. by lowering the duty in proportion to $f_{app}/(f_{app} + f^-_{app} + g_{app})$. High duty ratios of 0.88 (Huxley 1957) and 0.75 (Brenner 1988) are calculated from the values of f and g for fast skeletal muscle fibres at maximally activating [Ca^{2+}]. Because P_i is always present under physiological conditions in intact fibres and P_i can accumulate in skinned fibres, the duty ratio at nominal P_i-free conditions like in myofibrils could be even higher than these values. However, the calculation of the duty ratio based on these simple 2-step mass action models assumes that (1) all compliance of the Ca^{2+} activated sarcomere resides in the cross-bridge, and (2) all cross-bridges participate in cycling. Both are likely not the case because of filament compliance and geometric constraints in the sarcomere which might partly explain the lower duty ratio of 0.33 evaluated from accurate stiffness measurements at different sarcomere length (Linari et al. 2007). The effect of the 3-D lattice organisation on restricting acto-myosin binding has been recently modelled in (Mijailovich et al. 2016).

Another explanation for slow force responses upon [P_i] changes would be that the P_i release is not a classical rapid equilibrium. Structurally, P_i release can be described by the backdoor release mechanism (Yount et al. 1995; Llinas et al. 2015). It has been proposed that the P_i is not released immediately after leaving the active site and may stay for significant time in the backdoor release tunnel (Houdusse and Sweeney 2016). How the delayed backdoor release and the potential rebinding of P_i to the active site would modulate force kinetics is not clear yet. However, high energy barriers for backdoor release and rebinding of P_i could explain why P_i release and P_i binding are coupled to the rate-limiting forward step $f^{\rightarrow}$ and its reversal $f^{\Downarrow}$, respectively. Alternatively, P_i release per se and $f^{\rightarrow}$ might be rapid but P_i release be still coupled to the rate-limiting transition f if P_i release only occurs from a very rare cross-bridge configuration or little occupied pre-P_i release state (A_0) (Geeves and Holmes 2005). In such a scenario, the likelihood (rate) of P_i release and thus f is limited by the low occupancy of A_0 because f relates to the product of the forward step $f^{\rightarrow}$ of P_i release and [A_0]. If [A_0] is low, P_i release per se ($f^{\rightarrow}$) might be fast but the rate of P_i release (f) still be rate-limiting.

Finally, it needs to be explained why slow force responses probed by [P_i] changes kinetically differ from fast force responses probed by small length changes, the so called 'force recovery'. While cross-bridges undergo a slow structural change or adopt a rare configuration for enabling P_i release and priming de novo force-generation during the ATPase cycle, force re-generation in contrast reflects a fast process uncoupled from the ATPase cycle that occurs from already primed states without need to resemble the slow structural change or adopt the rare configuration coupled to P_i release (Caremani et al. 2013). Both force generating processes take place in the cross-bridge cycle. Finding the link between the two processes will be an important goal in muscle research. Complete understanding of the cross-bridge mechanism will require identification and characterization of the intermediates involved in both processes.

Taken together, the slow kinetics of force rise upon [P_i] decrease in cardiac myofibril studies indicate that P_i release is strongly coupled to the same rate-limiting transition that determines de novo force generation upon Ca^{2+} activation and redistribution of cross-bridges upon large mechanical perturbations. For this reason, it is not possible to derive a preferential sequence of force-generation and P_i release from the force kinetics induced by P_i jumps (Stehle 2017). As stated before, a limitation to this conclusion is the still unresolved puzzle posed by the asymmetric P_i jumps found in fast muscle (and slow skeletal muscle at high temperature) that awaits experimental elucidation.

In contrast to slow force kinetics induced by [P_i] decrease and large mechanical perturbations, investigations by Lombardi and coworkers show that upon small mechanical perturbations, cross-bridges can rapidly and repeatedly regenerate force uncoupled from P_i release (Irving et al. 1992; Lombardi et al. 1992; Piazzesi et al. 1997; Caremani et al. 2008, 2013; Linari et al. 2010). In combination, de novo force generation appears to be limited by slow P_i release, whereas force can be rapidly regenerated independent from P_i release. The mechanisms underlying the coupling of P_i release and the rate-limiting transition for de novo force generation and the uncoupling of the force-generating step and P_i release for force *re*-generation needs still to be clarified. Solving these mechanisms and working towards a unifying concept combining turnover and recovery kinetics is essential for understanding the cross-bridge cycle and for developing drugs targeting the rate of skeletal and cardiac muscle contraction.

Acknowledgements RS is grateful for support by the German Research Foundation (FOR1352-TP09) and Köln Fortune (Faculty of Medicine, Cologne). This work was supported by Telethon Italy (GGP16191), Italian Ministry of Health (WFR GR-2011-02350583) and Università degli studi di Firenze (ex-60%) to CT. The authors thank Dr. Nicoletta Piroddi and Corrado Poggesi for helpful discussions. We acknowledge the seminal work of Prof. Dr. Bernhard Brenner on rate-modulation of k_{TR} and its impact for the cross-bridge mechanism.

References

Araujo A, Walker JW (1996) Phosphate release and force generation in cardiac myocytes investigated with caged phosphate and caged calcium. Biophys J 70:2316–2326

Belus A, Piroddi N, Tesi C (2003) Mechanism of cross-bridge detachment in isometric force relaxation of skeletal and cardiac myofibrils. J Muscle Res Cell Motil 24:261–267

Bershitsky SY, Tsaturyan AK (2002) The elementary force generation process probed by temperature and length perturbations in muscle fibres from the rabbit. J Physiol 540:971–988

Bowater R, Sleep J (1988) Demembranated muscle fibers catalyze a more rapid exchange between phosphate and adenosine triphosphate than actomyosin subfragment 1. BioChemistry 27:5314–5323

Brenner B (1988) Effect of Ca^{2+} on cross-bridge turnover kinetics in skinned single rabbit psoas fibers: implications for regulation of muscle contraction. Proc Natl Acad Sci USA 85:3265–3269

Brenner B, Chalovich JM (1999) Kinetics of thin filament activation probed by fluorescence of *N*-((2-(iodoacetoxy)ethyl)-*N*-methyl) amino-7-nitrobenz-2-oxa-1, 3-diazole-labeled troponin I incorporated into skinned fibers of rabbit psoas muscle: implications for regulation of muscle contraction. Biophys J 77:2692–2708

Brenner B, Eisenberg E (1986) Rate of force generation in muscle: correlation with actomyosin ATPase activity in solution. Proc Natl Acad Sci USA 83:3542–3546

Campbell KS (2016) Compliance accelerates relaxation in muscle by allowing myosin heads to move relative to actin. Biophys J 110:661–668

Capitanio M, Canepari M, Cacciafesta P, Lombardi V, Cicchi R, Maffei M, Pavone FS, Bottinelli R (2006) Two independent mechanical events in the interaction cycle of skeletal muscle myosin with actin. Proc Natl Acad Sci USA 103:87–92

Caremani M, Dantzig J, Goldman YE, Lombardi V, Linari M (2008) Effect of inorganic phosphate on the force and number of myosin cross-bridges during the isometric contraction of permeabilized muscle fibers from rabbit psoas. Biophys J 95:5798–5808

Caremani M, Melli L, Dolfi M, Lombardi V, Linari M (2013) The working stroke of the myosin II motor in muscle is not tightly coupled to release of orthophosphate from its active site. J Physiol 591:5187–5205

Caremani M, Melli L, Dolfi M, Lombardi V, Linari M (2015) Force and number of myosin motors during muscle shortening and the coupling with the release of the ATP hydrolysis products. J Physiol 593:3313–3332

Chalovich JM, Eisenberg E (1982) Inhibition of actomyosin ATPase activity by troponin-tropomyosin without blocking the binding of myosin to actin. J Biol Chem 257:2432–2437

Colomo F, Poggesi C, Tesi C (1994) Force responses to rapid length changes in single intact cells from frog heart. J Physiol 475:347–350

Colomo F, Piroddi N, Poggesi C, te Kronnie G, Tesi C (1997) Active and passive forces of isolated myofibrils from cardiac and fast skeletal muscle of the frog. J Physiol 500:535–548

Colomo F, Nencini S, Piroddi N, Poggesi C, Tesi C (1998) Calcium dependence of the apparent rate of force generation in single striated muscle myofibrils activated by rapid solution changes. Adv Exp Med Biol 453:373–381

Cooke R (1997) Actomyosin interaction in striated muscle. Physiol Rev 77:671–697

Cooke R, Franks K, Luciani GB, Pate E (1988) The inhibition of rabbit skeletal muscle contraction by hydrogen ions and phosphate. J Physiol 395:77–97

Coupland ME, Ranatunga KW (2003) Force generation induced by rapid temperature jumps in intact mammalian (rat) skeletal muscle fibres. J Physiol 548:439–449

Dantzig JA, Goldman YE, Millar NC, Lacktis J, Homsher E (1992) Reversal of the cross-bridge force-generating transition by photogeneration of phosphate in rabbit psoas muscle fibres. J Physiol 451:247–278

Davis JS, Rodgers ME (1995) Indirect coupling of phosphate release to de novo tension generation during muscle contraction. Proc Natl Acad Sci USA 92:10482–10486

de Tombe PP, Stienen GJ (2007) Impact of temperature on cross-bridge cycling kinetics in rat myocardium. J Physiol 584:591–600

Dong C, Chen B (2016) Temperature effect on the chemomechanical regulation of substeps within the power stroke of a single Myosin II. Sci Rep 6:19506

Edes IF, Czuriga D, Csanyi G, Chlopicki S, Recchia FA, Borbely A, Galajda Z, Edes I, van der Velden J, Stienen GJ, Papp Z (2007) Rate of tension redevelopment is not modulated by sarcomere length in permeabilized human, murine, and porcine cardiomyocytes. Am J Physiol Regul Integr Comp Physiol 293:R20-29

Edman KA, Flitney FW (1982) Laser diffraction studies of sarcomere dynamics during 'isometric' relaxation in isolated muscle fibres of the frog. J Physiol 329:1–20

Eisenberg E, Greene LE (1980) The relation of muscle biochemistry to muscle physiology. Annu Rev Physiol 42:293–309

Eisenberg E, Hill TL (1985) Muscle contraction and free energy transduction in biological systems. Science 227:999–1006

Finer JT, Simmons RM, Spudich JA (1994) Single myosin molecule mechanics: piconewton forces and nanometre steps. Nature 368:113–119

Ford LE, Huxley AF, Simmons RM (1977) Tension responses to sudden length change in stimulated frog muscle fibres near slack length. J Physiol 269:441–515

Fortune NS, Geeves MA, Ranatunga KW (1991) Tension responses to rapid pressure release in glycerinated rabbit muscle fibers. Proc Natl Acad Sci USA 88:7323–7327

Geeves MA (2016) Review: The ATPase mechanism of myosin and actomyosin. Biopolymers 105:483–491

Geeves MA, Holmes KC (2005) The molecular mechanism of muscle contraction. Adv Protein Chem 71:161–193

Gordon AM, Homsher E, Regnier M (2000) Regulation of contraction in striated muscle. Physiol Rev 80:853–924

Hibberd MG, Webb MR, Goldman YE, Trentham DR (1985a) Oxygen exchange between phosphate and water accompanies calcium-regulated ATPase activity of skinned fibers from rabbit skeletal muscle. J Biol Chem 260:3496–3500

Hibberd MG, Dantzig JA, Trentham DR, Goldman YE (1985b) Phosphate release and force generation in skeletal muscle fibers. Science 228:1317–1319

Houdusse A, Sweeney HL (2016) How myosin generates force on actin filaments. Trends Biochem Sci 41:989–997

Huxley AF (1957) Muscle structure and theories of contraction. Prog Biophys Biophys Chem 7:255–318

Huxley HE (2004) Recent X-ray diffraction studies of muscle contraction and their implications. Philos Trans R Soc Lond B Biol Sci 359:1879–1882

Irving M, Lombardi V, Piazzesi G, Ferenczi MA (1992) Myosin head movements are synchronous with the elementary force-generating process in muscle. Nature 357:156–158

Kawai M, Halvorson HR (1991) Two step mechanism of phosphate release and the mechanism of force generation in chemically skinned fibers of rabbit psoas muscle. Biophys J 59:329–342

Kerrick WG, Xu Y (2004) Inorganic phosphate affects the pCa-force relationship more than the pCa-ATPase by increasing the rate of dissociation of force generating cross-bridges in skinned fibers from both EDL and soleus muscles of the rat. J Muscle Res Cell Motil 25:107–117

Linari M, Caremani M, Piperio C, Brandt P, Lombardi V (2007) Stiffness and fraction of Myosin motors responsible for active force in permeabilized muscle fibers from rabbit psoas. Biophys J 92:2476–2490

Linari M, Caremani M, Lombardi V (2010) A kinetic model that explains the effect of inorganic phosphate on the mechanics and

energetics of isometric contraction of fast skeletal muscle. Proc Biol Sci 277:19–27

Llinas P, Isabet T, Song L, Ropars V, Zong B, Benisty H, Sirigu S, Morris C, Kikuti C, Safer D, Sweeney HL, Houdusse A (2015) How actin initiates the motor activity of myosin. Dev Cell 33:401–412

Lombardi V, Piazzesi G, Linari M (1992) Rapid regeneration of the actin-myosin power stroke in contracting muscle. Nature 355:638–641

Lopez-Davila AJ, Elhamine F, Ruess DF, Papadopoulos S, Iorga B, Kulozik FP, Zittrich S, Solzin J, Pfitzer G, Stehle R (2012) Kinetic mechanism of Ca^{2+}-controlled changes of skeletal troponin I in psoas myofibrils. Biophys J 103:1254–1264

Lymn RW, Taylor EW (1971) Mechanism of adenosine triphosphate hydrolysis by actomyosin. BioChemistry 10:4617–4624

Mansfield C, West TG, Curtin NA, Ferenczi MA (2012) Stretch of contracting cardiac muscle abruptly decreases the rate of phosphate release at high and low calcium. J Biol Chem 287:25696–25705

Mansson A (2016) Actomyosin based contraction: one mechanokinetic model from single molecules to muscle? J Muscle Res Cell Motil 37:181–194

Mansson A, Rassier D, Tsiavaliaris G (2015) Poorly understood aspects of striated muscle contraction. Biomed Res Int 2015:245154

Martin H, Bell MG, Ellis-Davies GC, Barsotti RJ (2004) Activation kinetics of skinned cardiac muscle by laser photolysis of nitrophenyl-EGTA. Biophys J 86:978–990

Mijailovich SM, Kayser-Herold O, Stojanovic B, Nedic D, Irving TC, Geeves MA (2016) Three-dimensional stochastic model of actin-myosin binding in the sarcomere lattice. J Gen Physiol 148:459–488

Mijailovich SM, Nedic D, Svicevic M, Stojanovic B, Walklate J, Ujfalusi Z, Geeves MA (2017) Modeling the actin.myosin ATPase cross-bridge cycle for skeletal and cardiac muscle myosin isoforms. Biophys J 112:984–996

Millar NC, Homsher E (1990) The effect of phosphate and calcium on force generation in glycerinated rabbit skeletal muscle fibers. A steady-state and transient kinetic study. J Biol Chem 265:20234–20240

Millar NC, Homsher E (1992) Kinetics of force generation and phosphate release in skinned rabbit soleus muscle fibers. Am J Physiol 262:C1239-1245

Muretta JM, Rohde JA, Johnsrud DO, Cornea S, Thomas DD (2015) Direct real-time detection of the structural and biochemical events in the myosin power stroke. Proc Natl Acad Sci USA 112:14272–14277

Palmer S, Kentish JC (1998) Roles of Ca^{2+} and crossbridge kinetics in determining the maximum rates of Ca^{2+} activation and relaxation in rat and guinea pig skinned trabeculae. Circ Res 83:179–186

Pate E, Cooke R (1989) A model of crossbridge action: the effects of ATP, ADP and P_i. J Muscle Res Cell Motil 10:181–196

Piazzesi G, Linari M, Reconditi M, Vanzi F, Lombardi V (1997) Cross-bridge detachment and attachment following a step stretch imposed on active single frog muscle fibres. J Physiol 498:3–15

Piroddi N, Tesi C, Pellegrino MA, Tobacman LS, Homsher E, Poggesi C (2003) Contractile effects of the exchange of cardiac troponin for fast skeletal troponin in rabbit psoas single myofibrils. J Physiol 552:917–931

Poggesi C, Tesi C, Stehle R (2005) Sarcomeric determinants of striated muscle relaxation kinetics. Pflugers Arch 449:505–517

Potma EJ, van Graas IA, Stienen GJ (1995) Influence of inorganic phosphate and pH on ATP utilization in fast and slow skeletal muscle fibers. Biophys J 69:2580–2589

Ranatunga KW, Coupland ME, Mutungi G (2002) An asymmetry in the phosphate dependence of tension transients induced by length perturbation in mammalian (rabbit psoas) muscle fibres. J Physiol 542:899–910

Regnier M, Homsher E (1998) The effect of ATP analogs on posthydrolytic and force development steps in skinned skeletal muscle fibers. Biophys J 74:3059–3071

Regnier M, Morris C, Homsher E (1995) Regulation of the crossbridge transition from a weakly to strongly bound state in skinned rabbit muscle fibers. Am J Physiol 269:C1532–C1539

Siththanandan VB, Donnelly JL, Ferenczi MA (2006) Effect of strain on actomyosin kinetics in isometric muscle fibers. Biophys J 90:3653–3665

Smith DA (2014) A new mechanokinetic model for muscle contraction, where force and movement are triggered by phosphate release. J Muscle Res Cell Motil 35:295–306

Smith D, Sleep J (2006) Strain-dependent kinetics of the myosin working stroke, and how they could be probed with optical-trap experiments. Biophys J 91:3359–3369

Solzin J, Iorga B, Sierakowski E, Gomez Alcazar DP, Ruess DF, Kubacki T, Zittrich S, Blaudeck N, Pfitzer G, Stehle R (2007) Kinetic mechanism of the Ca^{2+}-dependent switch-on and switch-off of cardiac troponin in myofibrils. Biophys J 93:3917–3931

Steffen W, Sleep J (2004) Using optical tweezers to relate the chemical and mechanical cross-bridge cycles. Philos Trans R Soc Lond B Biol Sci 359:1857–1865

Stehle R (2017) Force responses and sarcomere dynamics of cardiac myofibrils induced by rapid changes in $[P_i]$. Biophys J 112:356–367

Stehle R, Kruger M, Scherer P, Brixius K, Schwinger RH, Pfitzer G (2002a) Isometric force kinetics upon rapid activation and relaxation of mouse, guinea pig and human heart muscle studied on the subcellular myofibrillar level. Basic Res Cardiol 97:I127–I135

Stehle R, Kruger M, Pfitzer G (2002b) Force kinetics and individual sarcomere dynamics in cardiac myofibrils after rapid Ca^{2+} changes. Biophys J 83:2152–2161

Stehle R, Solzin J, Iorga B, Poggesi C (2009) Insights into the kinetics of Ca^{2+}-regulated contraction and relaxation from myofibril studies. Pflugers Arch 458:337–357

Takagi Y, Shuman H, Goldman YE (2004) Coupling between phosphate release and force generation in muscle actomyosin. Philos Trans R Soc Lond B Biol Sci 359:1913–1920

Telley IA, Denoth J (2007) Sarcomere dynamics during muscular contraction and their implications to muscle function. J Muscle Res Cell Motil 28:89–104

Telley IA, Denoth J, Stussi E, Pfitzer G, Stehle R (2006) Half-sarcomere dynamics in myofibrils during activation and relaxation studied by tracking fluorescent markers. Biophys J 90:514–530

Tesi C, Colomo F, Nencini S, Piroddi N, Poggesi C (2000) The effect of inorganic phosphate on force generation in single myofibrils from rabbit skeletal muscle. Biophys J 78:3081–3092

Tesi C, Colomo F, Piroddi N, Poggesi C (2002a) Characterization of the cross-bridge force-generating step using inorganic phosphate and BDM in myofibrils from rabbit skeletal muscles. J Physiol 541:187–199

Tesi C, Piroddi N, Colomo F, Poggesi C (2002b) Relaxation kinetics following sudden Ca^{2+} reduction in single myofibrils from skeletal muscle. Biophys J 83:2142–2151

Thomas DD, Kast D, Korman VL (2009) Site-directed spectroscopic probes of actomyosin structural dynamics. Annu Rev Biophys 38:347–369

Trentham DR, Bardsley RG, Eccleston JF, Weeds AG (1972) Elementary processes of the magnesium ion-dependent adenosine triphosphatase activity of heavy meromyosin. A transient kinetic approach to the study of kinases and adenosine triphosphatases and a colorimetric inorganic phosphate assay in situ. Biochem J 126:635–644

Veigel C, Bartoo ML, White DC, Sparrow JC, Molloy JE (1998) The stiffness of rabbit skeletal actomyosin cross-bridges determined with an optical tweezers transducer. Biophys J 75:1424–1438

Wahr PA, Rall JA (1997) Role of calcium and cross bridges in determining rate of force development in frog muscle fibers. Am J Physiol 272:C1664-1671

Wahr PA, Cantor HC, Metzger JM (1997) Nucleotide-dependent contractile properties of Ca^{2+}-activated fast and slow skeletal muscle fibers. Biophys J 72:822–834

Walker JW, Lu Z, Moss RL (1992) Effects of Ca^{2+} on the kinetics of phosphate release in skeletal muscle. J Biol Chem 267:2459–2466

Wang L, Kawai M (2013) A re-interpretation of the rate of tension redevelopment k_{TR} in active muscle. J Muscle Res Cell Motil 34:407–415

Webb MR, Hibberd MG, Goldman YE, Trentham DR (1986) Oxygen exchange between P_i in the medium and water during ATP hydrolysis mediated by skinned fibers from rabbit skeletal muscle. Evidence for P_i binding to a force-generating state. J Biol Chem 261:15557–15564

Yount RG, Lawson D, Rayment I (1995) Is myosin a "back door" enzyme? Biophys J 68:44S–47S **(discussion 47S–49S)**